COMSOL-based Simulations of Criticality Excursion Transients in Fissile Solution

Christopher J. Hurt[*,1], Peter L. Angelo[2], Ronald E. Pevey[1]
[1]University of Tennessee, Department of Nuclear Engineering
[2]Y-12 National Security Complex, Safety Analysis Engineering
*Corresponding author: P. O. Box 2008, Oak Ridge, TN 37831-6399, churt2@utk.edu, cjh@ornl.gov

Abstract: Simulation of criticality accident transients offers the ability to confirm understanding of critical configurations, bound accident scenarios and aid comprehensive emergency planning. Computational ability to recreate excursion power histories in fissile solution is sought due to the predominance of fissile solutions in process criticality accidents [1]. Applicable solution transient physics methodologies are developed for neutron kinetics, heat transfer, and radiolytic gas transport.

This work is the first step in validating the use of COMSOL [2] as a flexible and powerful computational tool to simulate criticality excursions. Previously, characterization of excursion power history profiles has been limited to hand-calculations and simulation tools with 1-D/0-D physics treatments for specific geometries [3, 4, 5, 6]. This work demonstrates COMSOL's capability for an accurate, generalized approach to excursion simulations for nuclear safety applications.

Keywords: SILENE, neutronics, multiphysics, transport.

1. Introduction

COMSOL Multiphysics is used to develop coupled physics for radiolytic gas transport, neutron kinetics, and heat transfer for the purpose of simulating criticality excursion power histories. This simulation tool is exhibited for two cases: a documented criticality benchmark experiment, SILENE LE1-641 [3] and a theoretical configuration.

1.2 Brief Criticality Excursion Background

A critical, or supercritical, configuration of fissionable material is said to be present when the fission chain reaction is self-sustaining. That is, when the ratio of fissions, or neutrons, from one generation to the next (called the effective neutron multiplication factor, k_{eff}, per Eq. 1) is equal to or greater than unity. Reactivity, ρ, is the measure of the deviation of k_{eff} from unity, or a critical state, (see Eq. 2). Reactivity is often expressed in terms of dollars and cents, where a dollar is equal to the delayed neutron fraction, β_{eff}. A criticality excursion occurs when this chain reaction experiences exponential growth until a "spike" occurs in the power history, due to a natural or external negative reactivity feedback effect.

$$k_{eff} = \frac{\text{neutrons in generation i}}{\text{neutrons in generation i-1}} \quad \textbf{(1)}$$

$$\rho = \frac{k_{eff}-1}{k_{eff}} \quad \textbf{(2)}$$

For a fissile solution excursion, there are several multiphysics phenomena which naturally serve as the reactivity feedback to dampen a power excursion. The first feedback considered in this study is the rise in temperature, which affects both the density and nuclear properties of materials, and the second the phenomena of radiolysis, where gas bubbles are formed due to fission particle tracks.

1.3 SILENE LE1-641

The SILENE LE1-641 benchmark was part of a series of criticality experiments performed at the SILENE reactor at the Valduc Laboratory Critical Experiment Facilities in France. The SILENE reactor is an annular, cylindrical tank with an outer chamber for fissile solution and an inner chamber for control rod insertion. Figure 1 shows a picture and diagram of the SILENE reactor.

The SILENE LE1-641 benchmark consists of a 93% enriched uranyl nitrate (UN) solution, in which reactivity is inserted via the rapid withdrawal of a control rod. This results in a 2$ reactivity insertion over the first 20 seconds of the transient.

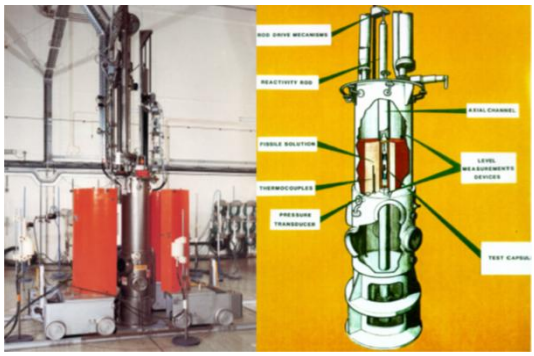

Figure 1. Image and diagram of SILENE.

1.4 "Methodological" Exercise

The "Methodological" or theoretical exercise was devised by the Organisation for Economic Co-operation and Development Nuclear Energy Agency's Criticality Excursions Analyses Expert Group as a preliminary study. It consists of an open, rectangular stainless steel container with UN solution. It is analyzed for multiple criticality configurations.

2. Use of COMSOL Multiphysics

COMSOL version 4.3 was used for the simulations presented here. The multiphysics methodology can be described in three different domains: the neutron kinetics, conjugate heat transfer and radiolytic gas transport. The nuclear data parameters and reactivity feedbacks necessary for input into the neutron point kinetics equations were derived by MCNP5 [7], a 3-D, Monte Carlo particle transport code.

The SILENE reactor was modeled in COMSOL using a 2-D axisymmetric geometry and the theoretical container a 3-D symmetrical quarter slice..

2.1 Point Kinetics

A full solution to a neutron transport problem considers the neutron flux in dimensions of energy, direction, space and time. Simplifications of this approach yield more computationally accessible governing equations by assuming a weak or non-dependence of the solution on these variables, among other assumptions. The neutron diffusion equations, previously used in COMSOL nuclear safety work [8], use a weak dependence on angle and energy. Arriving at the point kinetics equations [9] requires a further simplification that the total neutron flux is dependent only on time.

Seven equations are imported in the Global ODE application for point kinetics: six delayed one neutron balance equation (Eq. 3) and neutron precursor,, groups, $C_{i,}$,(Eq. 4). For convenience the excursion power, P, or fission rate, is substituted for the neutron flux – which is mathematically consistent as the two are proportional.

$$\frac{dP(t)}{dt} = \frac{\rho(t) - \beta_{eff}}{\Lambda} P(t) + \sum_{i=1}^{6} \lambda_i C_i(t) \qquad \textbf{(3)}$$

$$\frac{dC_i(t)}{dt} = \frac{\beta_i}{\Lambda} n(t) - \lambda_i C_i(t), \; i = 1,\ldots,6 \qquad \textbf{(4)}$$

The kinetic parameters β_i, Λ, and λ_i are the i^{th} precursor group delayed neutron fraction, mean neutron generation time and i^{th} grroup precursor decay rate, respectively, as calculated in MCNP5 [10].

Since the point kinetics equations do not consider the spatial distribution of the neutron flux, a fundamental cosine function is assumed for the flux, and confirmed for initial conditions in MCNP5. This is implemented as the driving force for volumetric heating and molecule/bubble production in the conjugate heat transfer and radiolytic gas transport physics, respectively.

The conjugate heat transfer and radiolytic gas transport applications interact with the point kinetics application via reactivity feedbacks averaged over the solution domain, as mentioned previously and shown in Eq. 5. The temperature, T, from the heat transfer solution decreases reactivity via density reduction and variation in nuclear data, while the radiolytic gas solution perturbs reactivity via the introduction of void bubble volume,. V.

$$\rho(t) = \rho_0 + ramp(t) + \alpha_T \Delta T + \alpha_V \Delta V \qquad \textbf{(5)}$$

The terms α_T and α_V are the feedback coefficients for temperature and void, respectively, implemented as interpolation functions in COMSOL and input from data derived in MCNP5. The ρ_0 and ramp terms represent the step and ramp reactivity insertions which are dependent on each case.

2.2 Conjugate Heat Transfer

Heat transfer, via conduction and convection, physics are treated by the built-in Conjugate Heat Transfer application module in COMSOL. The heat equation (Eq. 6) is solved for all domains in both cases.

$$\dot{\rho}C_p\left(\frac{\partial T}{\partial t}+u\cdot\nabla T\right)=\nabla\cdot(k\nabla T)+Q \qquad \textbf{(6)}$$

The velocity, u, is zero for solid domains, $\dot{\rho}$ is the material density, T is the temperature, k is the material thermal conductivity and t is time. The volumetric heat source, Q, is introduced for the solution domain according to the power distribution in the point kinetics module:

$$Q=\frac{Pw_e}{V}\prod_{i=1}^{n}\frac{\pi}{2}\cos\left(\frac{\pi x_i}{L_i}-\delta_i\right) \qquad \textbf{(7)}$$

V is the solution volume, w_e the energy released per fission. x_i, L_i, and δ_i are, respectively, the position, solution length and potential phase shift for the i^{th} dimension of the solution geometry.

Equations for mass continuity (Eq. 8) and incompressible Navier-Stokes momentum (Eq. 9) are solved for the flow in applicable fluid domains:

$$\frac{\partial\dot{\rho}}{\partial t}+\nabla\cdot(\dot{\rho}u)=0 \qquad \textbf{(8)}$$

$$\dot{\rho}\left(\frac{\partial u}{\partial t}+(u\cdot\nabla)u\right)=-\nabla p+\nabla\left(\mu(\nabla u+(\nabla u)^T)-\frac{2}{3}\mu(\nabla\cdot u)I\right)+F \qquad \textbf{(9)}$$

The pressure, p, is initially at standard atmospheric pressure, μ the material dynamic viscosity, and F is an external body force due to gravity: g_const*$\dot{\rho}$.

2.2.1 Boundary Conditions

For the SILENE reactor study, symmetrical boundary conditions for the flow and heat flux are specified at the axial centerline. Symmetry is similarly introduced for the theoretical container at the inside surfaces of the quarter slice geometry. Natural convective cooling, as built-in by COMSOL, is specified on all external boundaries of the geometry. Heat continuity is assumed for internal surfaces, with a built-in COMSOL relation for fluid-solid interfaces. The no slip condition (v=0) is considered at container walls and open boundary/zero pressure constraints are specified at the top surface of the fluid domains.

2.3 Radiolytic Gas Transport

When a fission occurs, radiation is released in the form of fission recoil particles, or nuclei, and other radiation including photons, ionized particles, and neutrons. In a UN solution, this radiation causes a disassociation of the molecules as it traverses the material, leaving behind, among others, gas molecules in its wake. At a certain critical concentration, the gas molecules begin to form void bubbles within the solution, which is referred to as radiolytic gas.

Three alternate developments were utilized to implement the radiolytic gas transport physics, each implemented over the UN solution domain only.

2.3.1 Global Equations

For all treatments, transport of radiolytic gas bubbles in directions transverse to the axial, or z, axis are ignored (i.e. only the transport to, and out of, the solution surface is considered). For implementation into the Global ODEs application, six axial sections are solved for both the bubble volume (Eq. 9) and molar concentration (Eq. 10) balance equations [4]:

$$\frac{\partial V_i}{\partial t}=v_e\frac{P(t)w_e}{6}\theta(C_i-C_0)-v_b(\omega)\frac{V_i}{\Delta z}+v_b(\omega)\frac{V_{i-1}}{\Delta z} \qquad \textbf{(9)}$$

$$\frac{\partial C_i}{\partial t}=G_H\gamma_i P(t)w_e-v_b(\omega)\frac{C_i}{\Delta z}+v_b(\omega)\frac{C_{i-1}}{\Delta z}-\frac{C_i}{\tau}$$

(10)

V_i and C_i denote the i^{th} radiolytic gas volume and concentrations, respectively, while i-1 denotes the previous axial section. Radiolytic gas properties v_e, G_H, and τ are, respectively, the energy-void transfer coefficient, molecular disassociation rate, and gas dissolution rate. Δz is the length of an axial section, γ_i is the i^{th} power

ratio and v_b the bubble velocity as a special function of the inverse reactor period, ω_i.

2.3.2 Transport of Diluted Species

The Transport of Diluted Species is a built-in COMSOL application well-suited to the purpose of radiolytic gas bubble and molecular transport. The governing equations (Eq.'s 11 and 12) then take on a form similar to Eq.'s 9 and 10, yet more rigorous in the finite-element scheme.

$$\frac{\partial V}{\partial t} + v_b \nabla V = v_e P(t) w_e \theta (C - C_0) \quad \textbf{(11)}$$

$$\frac{\partial C}{\partial t} + v_b \nabla C = G_H Q - \frac{C}{\tau} \quad \textbf{(12)}$$

The RHS of Eq.'s 11 and 12 are defined as reaction rates, the bubble velocity is zero in the transverse plane, and Q is the volumetric power distribution specified in Eq. 7.

2.3.3 Equation-Based Modeling

The Coefficient Form PDE application is used for the Equation-Based Modeling methodology. Its use is the same as seen in Eq.'s 11 and 12, serving as a verification of the Transport of Diluted Species methodology and offering a more flexible application for future improvements.

2.3.4 Boundary Conditions

For all three radiolytic gas transport methodologies the following assumptions are applicable either implicitly, for the global methodology, or explicitly. No flux is assumed on the boundaries of the solution container walls and the top surface of the solution acts as an outflow boundary.

2.4 Initial Conditions

The initial conditions for the point kinetics physics are assumed to be the steady-state critical values of the power and precursor concentrations (i.e. the solution to Eq.'s 3 & 4 with the time derivative set to zero). The initial conditions for the heat transfer physics are the initial temperature and pressure at approximately STP, with all fluid domains at rest. The radiolytic gas concentration and volume is initially set at zero.

3. Results of Simulations

The PARDISIO direct solver was utilized on a single core PC with 4 GB of RAM for all simulations. Multiple time-dependent study steps were used for each simulation, to require stricter variable time-stepping and higher relative tolerances on rapid transient periods of the simulation. Approximately 5 - 30 thousand mesh elements were used across the geometries and 20 - 100 thousand DOF were solved.

For the SILENE LE1-641 transient, the first power peak does not occur until around 10 seconds when the configuration becomes "prompt-critical", where only prompt neutrons control the fission chain reaction (see Eq. 3). The oscillatory power history behavior typical of a rapid reactivity insertion in fissile solution follows. Here, at the first minute or two of the transient, the formation and dispersal of radiolytic gas, and resulting reactivity perturbations, dominates the power history. At around 100 seconds in, the temperature reactivity feedback becomes sufficiently negative to return the configuration to a subcritical state ($k_{eff}<1$, $\rho<0$) and the excursion power subsequently falls off.

The measured benchmark values and COMSOL-based results for the first 300 seconds of the excursion power history show good agreement, as seem in Figure 2. In addition, key excursion history characteristics such as first peak fission yield, time to first peak, and first peak total energy agree within a factor of two. The reactivity behavior and contributions which drive the transient during the first 200 seconds of the SILENE LE1-641 transient are shown in Figure 3.

Figure 4 demonstrates the radiolytic gas transport (using the Transport of Diluted Species application and Eq.'s 11 and 12) for three different reference points in the transient. At t=10.9 seconds, just before the first transient spike, the radiolytic gas concentration has an ideal axial cosine distribution as there are no gas bubbles yet formed to transport the gas molecules. The subsequent stages, shown in Figure 4, at the downslope of the first peak and its minimum clearly display the production, transport, and surface dispersion of the radiolytic gas molecules.

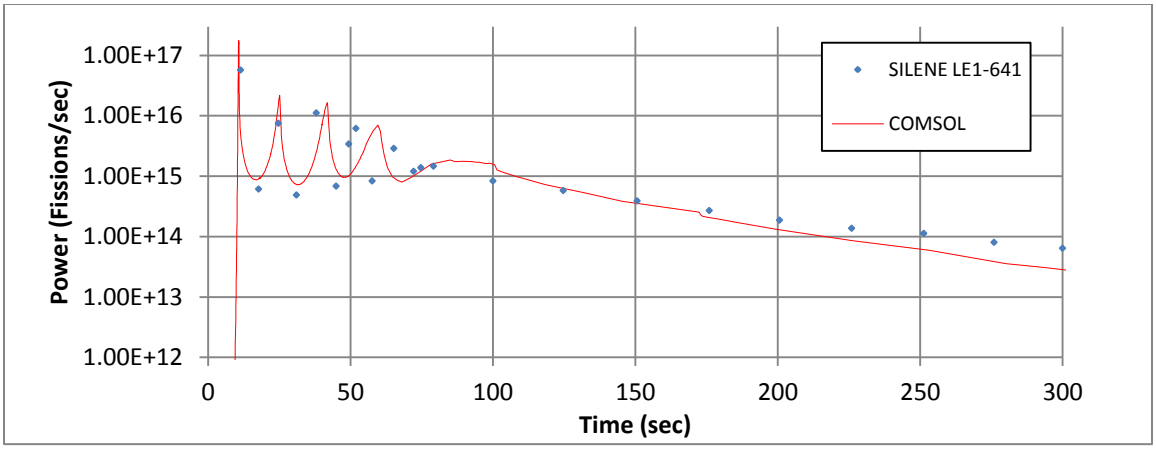

Figure 2: The excursion power (in fission/sec) during benchmark SILENE LE1-641.

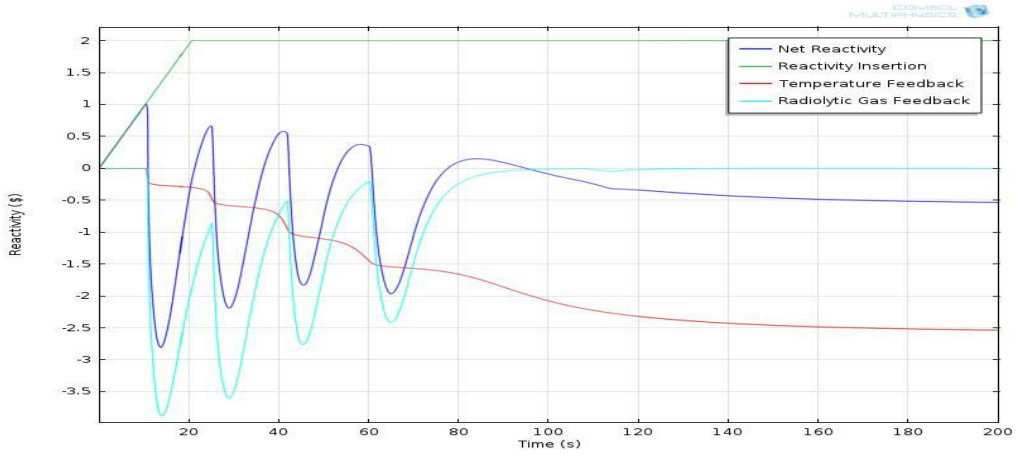

Figure 3: The reactivity contributions during benchmark SILENE LE1-641.

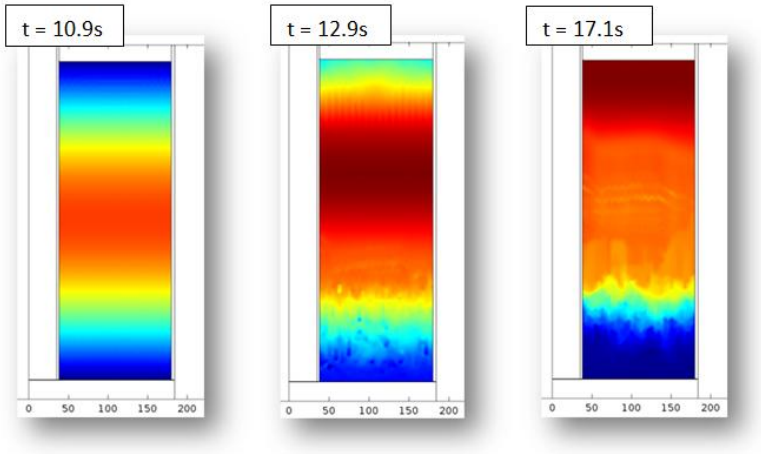

Figure 4: The radiolytic gas concentration during SILENE LE1-641 (dimensions in mm).

A second transient study considered is the response of the theoretical container to a 50 cent reactivity step at time=0. Because the system is supercritical by a reactivity margin less than the delayed neutron fraction the exponential growth of the transient is governed by the production of delayed neutrons (Eq. 4) and thus the excursion peak is considerably more gradual than the transient seen in SILENE LE1-641 (Fig. 1). Furthermore, as is expected, there is a single, smaller excursion peak dampened primarily by the temperature reactivity feedback with a small acceleration due to radiolytic gas formation. The power excursion history and driving reactivity behavior over the first 900 seconds can be seen in Figures 5 and 6.

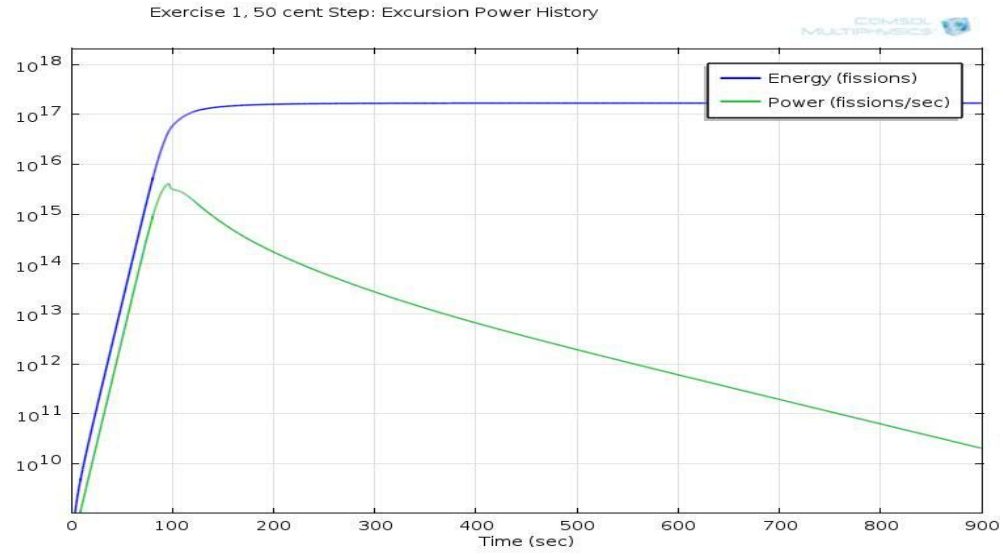

Figure 5: The excursion power (in fission/sec) and energy (fissions) for a 50¢ step in the theoretical container.

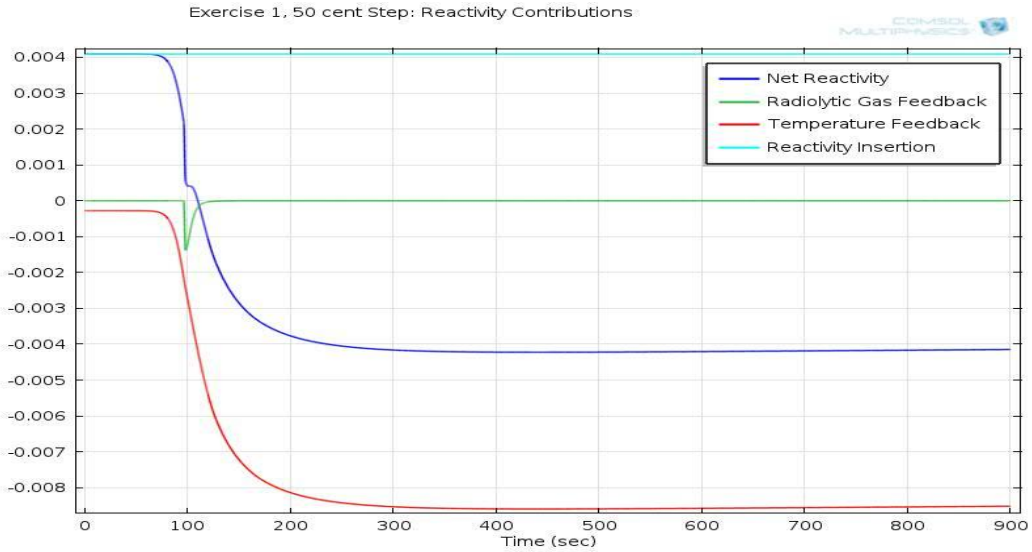

Figure 6: The reactivity contributions for a 50¢ step in the theoretical container.

4. Conclusions

Neutron kinetics, heat transfer and radiolytic gas transport physics methodologies were developed in COMSOL version 4.3 to solve the highly multiphysics phenomena of criticality power excursions in fissile solution. These methodologies were applied to two cases, criticality experiment SILENE LE1-641 and a theoretical exercise in 2-D axisymmetric and 3-D quarter slice geometries, respectively. The basic nuclear data were calculated with the MCNP5 neutron transport code.

This work demonstrates the accuracy and power of modeling criticality excursion transients using existing COMSOL modeling applications, and thus encourages extension into other accident scenarios (i.e. different geometries and fissile materials). In addition, improvements to the model are still ongoing which include the development of other physics which affect the excursion power history (e.g. solution sloshing and boiling) and enhancements to existing physics methodologies (e.g. space-time neutron kinetics and a higher fidelity radiolytic gas transport module).

5. References

1. MCLAUGHLIN, T., MONAHAN, S., PRUVOST, N., FROLOV, V., RYAZANOV, B., SVIRIDOV. I., "A Review of Criticality Accidents: 2000 revision" Report LA-13638, Los Alamos National Laboratory (2000)
2. COMSOL, Inc., "COMSOL Multiphysics User's Guide," Version 4.3, Burlington, MA (2012)
3. MIYOSHI, Y., et. al., "Inter-code Comparison Exercise for Criticality Excursion Analysis," NEA No. 6285, Nuclear Energy Agency, Organisation of Economic Co-operation and Development (2009)
4. BASOGLU, B., YAMAMOTO, T., OKUNO, H., NOMURA, Y.,"Development of a New Simulation Code for Evaluation of Criticality Transients Involving Fissile Solution Boiling," JAERI-Data/Code-98-011, Japan Atomic Energy Institute (1998)
5. MATHER, D., BUCKLEY, A., PRESCOTT, A., Critex: "A Code to Calculate the Fission Release Arising from Transient Criticality in Fissile Solutions," SRD R 380, AEA Technology (1994)
6. "Assessment of the TRACE Code Using Transient Data from Maanshan PWR Nuclear Power Plant," NUREG/IA-0241, U.S. Nuclear Regulatory Commission, Washington, D.C. (2010)
7. X-5 Monte Carlo Team, *MCNP—A General Monte Carlo N-Particle Transport Code*, Version 5, LA-CP-03-0245, Los Alamos National Laboratory (2003)
8. CHANDLER, D., *Spatially-Dependent Reactor Kinetics and Supporting Physics Validation Studies at the High Flux Isotope Reactor*, PhD Diss., University of Tennessee (2011)
9. KIEDROWSKI, B., et. al., MCNP5-1.6, *Feature Enhancements and Manual Clarifications*, LA-UR-10-06217, Los Alamos National Laboratory, Los Alamos, N.M (2010)
10. STACEY, W., *Nuclear Reactor Physics*, p. 147, WILEY-VCH, Berlin, Germany (2007)

6. Acknowledgements

The studies documented in this paper were made possible by a research contract between the University of Tennessee Nuclear Engineering Department and the Y-12 National Security Complex. The author would also like to thank the American Nuclear Society's Nuclear Criticality Safety Division for its support via a student scholarship.